MEDICAL SCIENCE MONITOR

CLINICAL RESEARCH

e-ISSN 1643-3750
© Med Sci Monit, 2018; 24: 7869-7874
DOI: 10.12659/MSM.909064

Received: 2018.01.19
Accepted: 2018.02.13
Published: 2018.11.03

Expression of Bax/Bcl-2, TGF-β1, and Type III Collagen Fiber in Congenital Muscular Torticollis

Authors' Contribution:
Study Design A
Data Collection B
Statistical Analysis C
Data Interpretation D
Manuscript Preparation E
Literature Search F
Funds Collection G

ABD 1 Dianguo Li
BFG 2 Kelai Wang
CEG 3 Wei Zhang
BCF 1 Junfeng Wang

1 Department of Pediatric Surgery, 2nd Hospital of Shandong University, Jinan, Shandong, P.R. China
2 Department of Pediatric Surgery, Qilu Hospital of Shandong University, Jinan, Shandong, P.R. China
3 Radiology Department, 2nd Hospital of Shandong University, Jinan, Shandong, P.R. China

Corresponding Author: Dianguo Li, e-mail: dianguoli17@163.com
Source of support: This work was funded by the Shandong Province Young and Middle-Aged Scientists Research Awards Fund (Grant No. ZR2011HM069)

Background: This study investigated the expression of Bax/Bcl-2, TGF-β1 and type III collagen fiber in sternocleidomastoid of congenital muscular torticollis (CMT), and explored the possible mechanisms of fibrosis in sternocleidomastoid of CMT.

Material/Methods: The localization and expression of Bax, Bcl-2, TGF-β1, and type III collagen were detected in the control group and experimental group by using immunohistochemical staining method. The RT-PCR assay was used to measure the expression of TGF-β1 in the control group and experimental group.

Results: HE staining results showed that the collagen fiber in the experimental group had more abundant hyperplasia compared to the control group ($p<0.05$). Immunohistochemical staining results showed that the expression of Bax, Bax/Bcl-2, TGF-β1, and type III collagen in the experimental group was significantly increased compared to the control group ($p<0.01$). There were positive correlations between expression of Bax/Bcl-2 and TGF-β1, and between expression of TGF-β1 and type III collagen fiber ($p<0.05$, $r=0.32$ and 0.83, respectively). The RT-PCR results showed that the expression of TGF-β1 mRNA was also significantly elevated in the experimental group compared to the control group ($p<0.05$).

Conclusions: Increased muscular apoptosis may aggravate the formation of muscular fibrosis, which may be involved in the pathogenesis of sternocleidomastoid of CMT.

MeSH Keywords: bcl-2-Associated X Protein • Collagen Type III • Genes, bcl-2 • Torticollis

Full-text PDF: https://www.medscimonit.com/abstract/index/idArt/909064

Indexed in: [Current Contents/Clinical Medicine] [SCI Expanded] [ISI Alerting System] [ISI Journals Master List] [Index Medicus/MEDLINE] [EMBASE/Excerpta Medica] [Chemical Abstracts/CAS]

Background

In clinical practice, congenital muscular torticollis (CMT) is a common congenital malformation. The morbidity of CMT in infants ranges from 0.4% to 1.9%. However, there is no malformation when the infant is born. Lumps appears at about 10 days after birth, which gradually turns to one-sided sternocleidomastoid (SCM) contracture and fibrosis degeneration, the head deflects towards the diseased side, and torticollis appears [1–4]. This study observed the CMT sternocleidomastoid extra-cellular matrix type III collagen hyperplasia conditions and the expression of Bax/Bcl-2, TGF-β1, and TGF-β1 mRNA by using methods of immunohistochemistry staining and RT-PCR assay, respectively. This study also observed the correlations between type III collagen hyperplasia and Bax/Bcl-2a and TGF-β1. Finally, we explored the possible pathogenesis of sternocleidomastoid fibrosis in CMT.

Material and Methods

Specimen collection

We collected 29 cases of CMT patients undergoing surgical intervention in the 2nd Hospital of Shandong University from June 2010 to June 2012. Among the 29 cases, there were 21 males and 8 females, with an average age of 1.3 years old (experiment group). The other 8 cases were assigned as the control group, containing 5 males and 3 females, with average age of 1.2 years old. Parents of all patients signed the Patient Information Consent Form, and the study was conducted according to ethics requirements. After removing the specimens, they were immediately placed in liquid nitrogen and stored in –80°C. Then, the specimens were divided into 2 parts, one for immunohistochemical staining and the other part for the RT-PCR assay.

Main agents and instruments

Bax and Bcl-2 detection kits, mouse anti-human type III collagen monoclonal antibody, rabbit anti-mouse TGF-β1 monoclonal antibody, ready-to-use SABC immunohistochemistry staining kit, and DAB coloration kit were purchased from Wuhan Boster Bioengineering Company (Wuhan, China). An Olympus IX 81 motor-driven inverted microscope (Olympus, Japan) was used for image acquisition.

The column total RNA extraction kit was purchased from Shanghai Generay Biological Engineering Company (Shanghai, China). TIANScript cDNA first-strand synthesis kit and 2×Taq PCR Master Mix were purchased from Beijing Science and Technology Company (Beijing, China). TIANGEN primer TGF-β1 mRNA and β-intrinsic factor (β-actin) were provided by the Shanghai Biological Engineering Company (Shanghai, China).

HE and Immunohistochemical Staining

All specimens were fixed with 10% neutral formalin, paraffin-embedded, and serially sectioned at 3–4 μm thickness. Hematoxylin-eosin (HE) staining and immunohistochemical staining processes were: (1) dewaxing, hydration, blocking-up the EGPO by 0.3% H_2O_2 methanol solution; (2) non-immune serum blocking, adding the primary antibody and the second antibody, and the third antibody in sequence; (3) DAB coloration, hematoxylin re-dyeing, and transparent finalizing. We replaced the primary antibody and the second antibody with the phosphate buffer solution (PBS, pH=7.4) to conduct the negative control.

Brown areas were positive positions. We randomly chose 10 non-overlapping visual fields for each section under a microscope at 20× magnification. We used the Image-pro Plus 6.0 image analysis system (Media Cybernetics, Inc., Bethesda, MD, USA) for analysis of the immunohistochemical results of Bax, Bcl-2, TGF-β1, and type III collagen fiber, and we used the staining range and strength to calculate average optical density. Each section was assessed by 3 pathologists. The double-blind method was used and the mean value was the average optical density.

RT-PCR for expression of TGF-β1 mRNA

All specimens of sternocleidomastoid cells were processed the same as in the control and experiment groups: (1) Extraction of TGF-β1 mRNA; (2) Reverse transcription mRNA into cDNA; (3) PCR amplification; The length of the target gene bands was 342 bp. The primer sequences for TGF-β1 mRNA were: Forwards: 5'-GCCCTGGACACCAACTATTG-3', Reverse: 5'-TTTTAGCTGCACTTGCAGC C-3'; (4) 1.5% agarose-gel electrophoresis; and (5) The electrophoretic band density was analyzed by using Quantity One software (Bio-Rad Laboratories, Hercules, CA, USA). The density ratio of target gene product and the reference gene product (PCR ratio) was determined for the semi-quantitative analysis of expression of TGF-β1 mRNA.

Statistics analysis

All data are shown as mean value ± standard deviation ($\overline{\chi}$±SD). The differences between 2 samples, such as expression of Bax, Bcl-2, Bax/Bcl-2, TGF-β1 type III Collagen, were analyzed by using the *t* test. ANOVA was used for comparison among multiple groups. The association between 2 samples of Bax/Bcl-2, TGF-β1, and Type III collagen was analyzed by means of linear correlation. All statistical analysis was done using SPSS 13.0 statistics software (SPSS, Inc., Chicago, IL, USA). $p<0.05$ was considered as statistical significance.

Indexed in: [Current Contents/Clinical Medicine] [SCI Expanded] [ISI Alerting System] [ISI Journals Master List] [Index Medicus/MEDLINE] [EMBASE/Excerpta Medica] [Chemical Abstracts/CAS]

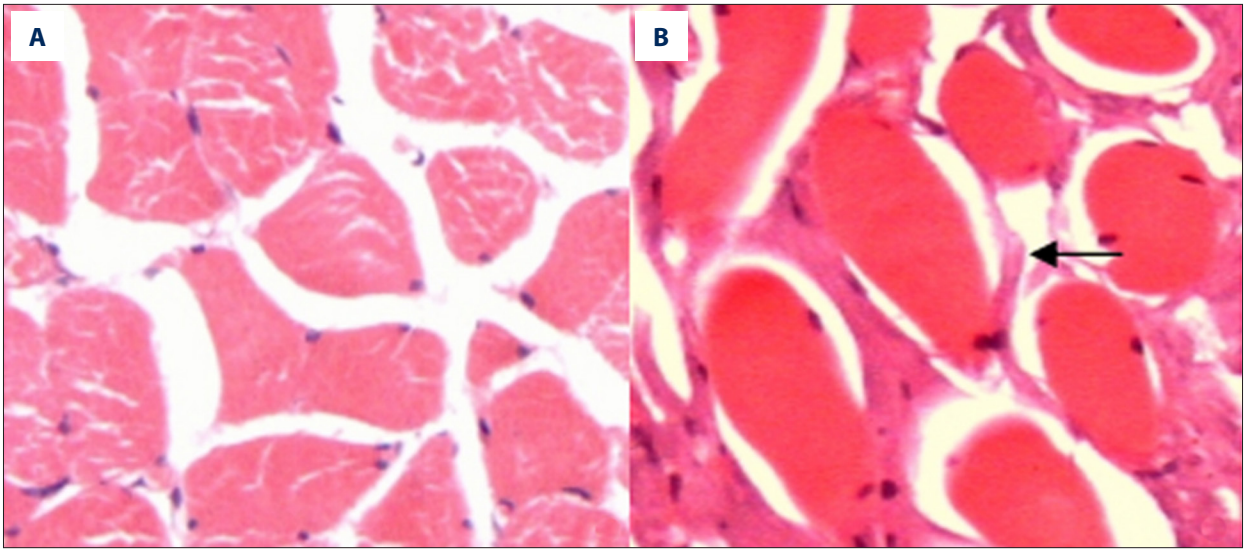

Figure 1. HE staining of control group (**A**), experimental group (**B**) (HE, ×200).

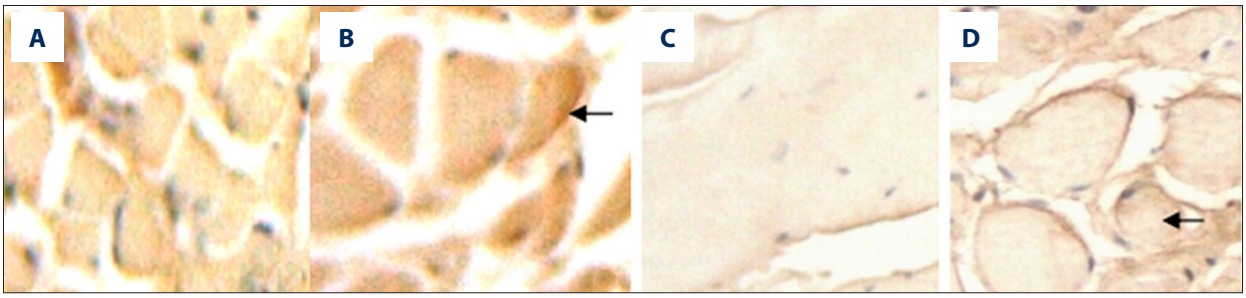

Figure 2. Bax staining of control group (**A**) and experiment group (**B**), and Bcl-2 staining of control group (**C**) and experiment group (**D**), (SP, ×200).

Results

HE Staining

In the control group, the muscle cells and muscle bundles ranks were orderly and regular. Collagen fiber were rare among the muscle cells and there was only a small amount of collagen fibers among the muscle bundles and surrounding the small blood vessels. In the experimental group, there were large amounts of collagen fibroplasias among the muscle bundles and cells (←). The muscle bundles and cells were arranged irregularly and muscle cells had varying degrees of atrophy (Figure 1).

Immunohistochemical staining observation

In the control group, few brown particles of Bax protein and Bcl-2 protein appeared in the cytoplasm, whereas abundant brown particles appeared in cytoplasm of the experimental group (some areas were platy (←), Figure 2). In the experimental group, average optical density values of both Bax protein and Bcl-2 protein were increased. However, the increasing range for the former was higher compared to the latter. The average optical density for Bax protein was significantly different between the control group and experimental group ($p<0.01$). There was no significant difference in average optical density of the Bcl-2 protein between the control group and experiment group. The average optical density for Bax/Bcl-2 of the experiment group was significantly higher compared to the control group (Table 1, $p<0.01$). There were no TGF-β1-positively staining cells in the cytoplasm of the control group, but cytoplasm of the experiment group had a dense platy expression (←). The average optical density for TGF-β1 in the experiment group was significantly higher compared to the experiment group ($p<0.01$). In the control group, only a small amount of type III collagen fiber was expressed among the muscle bundles; however, there was no expression among the muscle cells. In the experiment group, type III collagen fiber expression was significantly increased among muscle bundles and cells (←). Numerous type III collagen fibers were found surrounding the residual muscle cells (Figure 3). The average optical density for type III collagen fiber was significantly higher in the experiment group compared to the control group ($p<0.01$).

Indexed in: [Current Contents/Clinical Medicine] [SCI Expanded] [ISI Alerting System] [ISI Journals Master List] [Index Medicus/MEDLINE] [EMBASE/Excerpta Medica] [Chemical Abstracts/CAS]

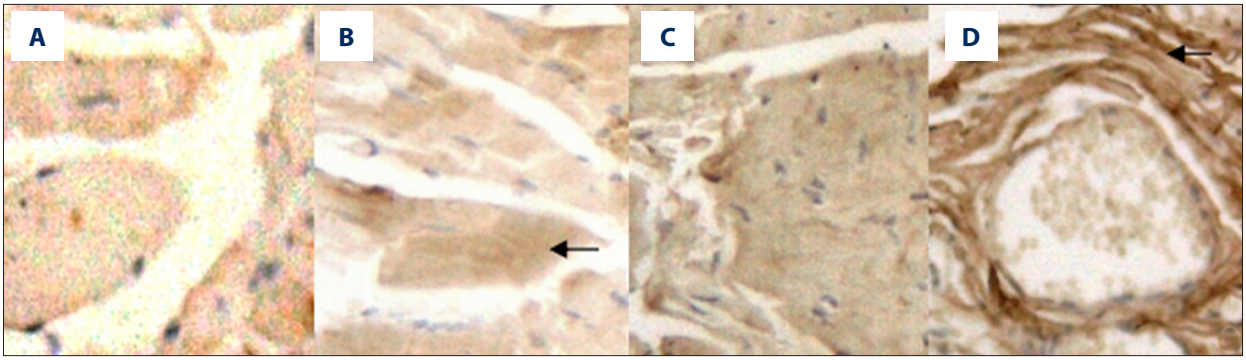

Figure 3. TGF-β1 staining of control group (**A**) and experiment group (**B**), and collagen type III Staining of control group (**C**) and experiment group (**D**), (SP, ×200).

Table 1. Average optical density value of Bax/Bcl-2, TGF-β1 and type III collagen ($\bar{\chi}$±s), * p<0.01.

Group	Case amount	Bax	Bcl-2	Bax/Bcl-2	TGF-β1	Type III collagen
Control	8	0.0795±0.0203	0.0523±0.0067	1.5182±0.0408	0.0450±0.0027	0.1818±0.002
Experiment	29	0.1719±0.0198*	0.0587±0.0082	2.9284±0.0200*	0.1956±0.0072*	0.3315±0.006*

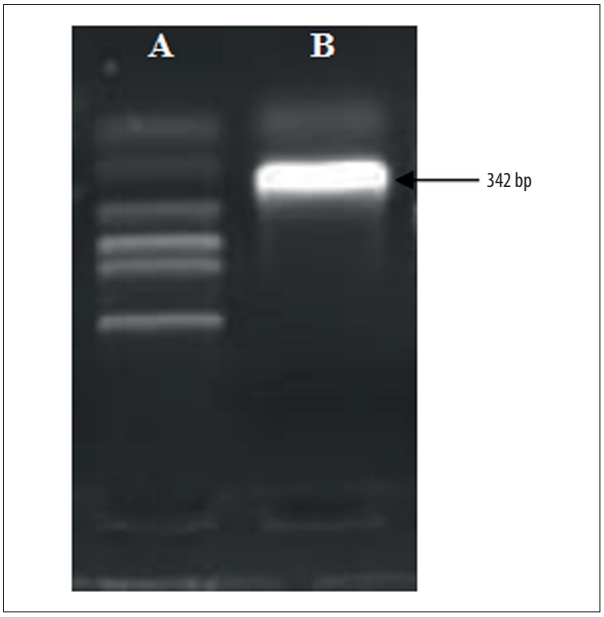

Figure 4. The electrophoretic band optical density for the control group 'A' and experimental group 'B'.

RT-PCR for the expression of TGF-β1 mRNA

The average gray value for the TGF-β1 mRNA levels in the experiment group (9.326±0.056) was significantly higher compared to the levels of TGF-β1 mRNA in the control group (0.886±0.032) (Table 1 and Figure 4, p<0.05).

Association between Bax/Bcl-2, TGF-β1, and type III collagen Fibers

Three sections from the same specimen were selected for immunohistochemical staining. The association between average optical densities in Bax/Bcl-2, TGF-β1, and type III collagen fibers was analyzed using the linear correlation method. The results showed that there were positive correlations between Bax/Bcl-2 and TGF-β1, and between TGF-β1 and Type III collagen fibers (r=0.32 and 0.83, respectively).

Discussions

The basic pathological change of CMT is stoma hyperplasia and fibrosis [5–7]. Over-deposition of the sternocleidomastoid extracellular matrix collagen and the other changes of extra-cellular matrixes may be the direct causes of the muscle fibrosis. The distribution of type III collagen is the widest in the tissues. Therefore, it is important to study the hyperplasia conditions of type III collagen in tissue fibrosis diseases and to discuss the relationships of all cell factors for type III collagen in the process of fibrosis diseases.

Bax and Bcl-2 belong to the Bcl-2 protein family, which comprises 2 large categories of proteins. Bcl-2 and Bax have anti-apoptosis and pro-apoptosis roles, respectively. The Bcl-2 protein family also includes other molecules, such as Bcl-xl and Bak. Bcl-2 and Bcl-xl are mainly distributed in the mitochondrial membranes, endoplasmic reticulum, and cytoplasm. Bax and Bak are mainly distributed in the cytoplasm. Previous studies

Indexed in: [Current Contents/Clinical Medicine] [SCI Expanded] [ISI Alerting System] [ISI Journals Master List] [Index Medicus/MEDLINE] [EMBASE/Excerpta Medica] [Chemical Abstracts/CAS]

found that, under the normal physiological state, Bax is mainly distributed in the cytoplasm. Under the influence of pro-apoptosis factors, Bax shifts from the cell cytoplasm to the mitochondria and forms channels with large-bore diameter at the mitochondrial outer membrane, which results in mitochondria membrane potential decrease and pro-apoptotic molecular action in mitochondria. Subsequently, the apoptosis process sets up [8–10], and finally activates caspase-3 and induces apoptosis [11]. As an apoptotic-resisting gene, Bcl-2 not only can inhibit the apoptosis caused by peroxide, but also can combine with Bax to form heterogonous dimers and participate in anti-oxidation reaction. When Bax is highly expressed, it can form Bax homodimer to promote cell apoptosis. When Bcl-2 is highly expressed, Bcl-2 and Bax can form heterogonous dimers to suppress apoptosis. Previous research has shown that the proportion of anti-apoptosis protein Bcl-2 and pro-apoptosis protein Bax decides whether apoptosis happens or not [12,13]. The above issues mean that if the Bax/Bcl-2 proportion increases, cell apoptosis is promoted, and vice versa. Bax/Bcl-2 proportion in the experiment group was significantly increased compared to the control group. Therefore, the apoptosis of skeletal muscle cells in the experiment group was higher compared to that of the control group. A previous [14] study verified that the apoptotic cells in CMT are myofibroblasts, which can secrete collagen and produce shrinkage. Furthermore, the myofibroblasts functions as both myofibroblasts and smooth muscle cells [14].

TGF-β is a large class of multi-functional cell growth and proliferation regulatory protein. TGF-β group comprises at least 6 molecules with relevant structure. TGF-β1 occupies the highest proportion in somatic cells (>90%) and it has the strongest activity. TGF-β1 is a cell factor generated by the strongest pro-fiber. Generally, there are few TGF-β1 in normal tissues. Constant immune injury or other factors can stimulate interstitial cells to secrete TGF-β1. Through autocrine or paracrine functions, the tissue secretes abundant extra-cellular matrix (ECM) and ECM degradation protease inhibitors, produces more ECM generation than degradation, and promotes ECM deposition [15]. Finally, it results in ECM increasing and fibrosis forming. In this study, the expression of TGF-β1 mRNA and protein in the experiment group was significantly higher compared to the control group. In the control group, there was little type III collagen expression among the muscle bundles and cells. In SCM fibrosis of CMT, the type III collagen expression was significantly increased, which can be seen among the muscle bundles and cells. There were also abundant type III collagen wrap muscle cells. With the increase of TGF-β1 expression, the expression of type III collagen is increased and the fibrosis degree is elevated.

Experimental results show a positive correlation between Bax/Bcl-2 and TGF-β1, and between TGF-β1 and type III collagen fibers. With the higher apoptosis of sternocleidomastoid, the TGF-β1 expression increases. Expression of type III collagen may further increase, and the fibrosis of sternocleidomastoid will be more significant. Therefore, apoptosis and TGF-β1 expression may play a key role in promoting sternocleidomastoid fibrosis. We found that, compared with the control group, Bax in the experiment group was significantly increased. The expression level for Bcl-2 was also increased, but it was not statistically significant compared to the control group. Our results show that in the fibrosis process, apoptosis and cell proliferation ability increase. It is generally thought that in the healthy state, cell apoptosis and proliferation maintain a dynamic balance. When sternocleidomastoid fibrosis appears with a large amount of cell apoptosis, the proliferation capacity of muscle cells has a compensatory increase to maintain the balance.

Conclusions

Deposition of type III collagen is a key factor in generating CMT sternocleidomastoid fibrosis. Its hyperplasia is associated with accelerated apoptosis and TGF-β1 over-expression. Therefore, in addition to the conservative or operative treatment, exploring new drugs to inhibit apoptosis, restricting TGF-β1 generation, blocking the signal transduction of TGF-β1, suppressing collagen generation, and promoting collagen degradation, may stop the sternocleidomastoid fibrosis in CMT forming the “source”.

Conflict of interest

None.

References:

1. Giray E, Karadag-Saygi E, Mansiz-Kaplan B et al: A randomized, single-blinded pilot study evaluating the effects of kinesiology taping and the tape application techniques in addition to therapeutic exercises in the treatment of congenital muscular torticollis. Clin Rehabil, 2017; 31: 1098–106
2. Hu CF, Fu TC, Chen CY et al: Longitudinal follow-up of muscle echotexture in infants with congenital muscular torticollis. Medicine, 2017; 96: e6068
3. Nilesh K, Mukherji S: Congenital muscular torticollis. Ann Maxillofac Surg, 2013; 3: 198–200
4. Lee K, Chung E, Lee BH: A study on asymmetry in infants with congenital muscular torticollis according to head rotation. J Phys Ther Sci, 2017; 29: 48–52
5. Lee YT, Cho SK, Yoon K et al: Risk factors for intrauterine constraint are associated with ultrasonographically detected severe fibrosis in early congenital muscular torticollis. J Pediatr Surg, 2011; 46: 514–19
6. Chen HX, Tang SP, Gao FT et al: Fibrosis, adipogenesis, and muscle atrophy in congenital muscular torticollis. Medicine, 2014; 93: e138

Indexed in: [Current Contents/Clinical Medicine] [SCI Expanded] [ISI Alerting System] [ISI Journals Master List] [Index Medicus/MEDLINE] [EMBASE/Excerpta Medica] [Chemical Abstracts/CAS]

7. Lee YT, Yoon K, Kim YB et al: Clinical features and outcome of physiotherapy in early presenting congenital muscular torticollis with severe fibrosis on ultrasonography: A prospective study. J Pediatr Surg, 2011; 46: 1526–31
8. Duensing TD, Watson SR: Assessment of apoptosis (programmed cell death) by flow cytometry. Cold Spring Harb Protoc, 2018; 2018: pdb prot093807
9. Zhang Z, Jin A, Yan D: MicroRNA206 contributes to the progression of steroidinduced avascular necrosis of the femoral head by inducing osteoblast apoptosis by suppressing programmed cell death 4. Mol Med Rep, 2018; 17: 801–8
10. Lindsay J, Esposti MD, Gilmore AP: Bcl-2 proteins and mitochondria – specificity in membrane targeting for death. Bioch Biophy Acta, 2011; 1813: 532–39
11. Glushakova OY, Glushakov AO, Borlongan CV et al: Role of Caspase-3-mediated apoptosis in chronic Caspase-3-cleaved tau accumulation and blood-brain barrier damage in the corpus callosum after traumatic brain injury in rats. J Neurotrauma, 2018; 35: 157–73
12. Shlezinger N, Irmer H, Dhingra S et al: Sterilizing immunity in the lung relies on targeting fungal apoptosis-like programmed cell death. Science, 2017; 357: 1037–41
13. Adams JM, Cory S: The BCL-2 arbiters of apoptosis and their growing role as cancer targets. Cell Death Different, 2018; 25: 27–36
14. Lee IJ, Lim SY, Song HS, Park MC: Complete tight fibrous band release and resection in congenital muscular torticollis. J Plast Reconstr Aesthet Surg, 2010; 63: 947–53
15. Ou L, Lin S, Song B et al: The mechanisms of graphene-based materials-induced programmed cell death: A review of apoptosis, autophagy, and programmed necrosis. Int J Nanomed, 2017; 12: 6633–46

Indexed in: [Current Contents/Clinical Medicine] [SCI Expanded] [ISI Alerting System] [ISI Journals Master List] [Index Medicus/MEDLINE] [EMBASE/Excerpta Medica] [Chemical Abstracts/CAS]